Journal of Statistical Physics, Vol. 76, Nos. 3/4, 1994

Vortex Phase Transitions in $2\frac{1}{2}$ Dimensions

Alexandre J. Chorin[1]

Received October 27, 1993

A phase diagram is mapped out for a "$2\frac{1}{2}$"-dimensional vortex lattice model in which vortex filaments lie in a plane, while both the velocity field and the Green function are three-dimensional. Both positive and negative temperatures are considered. Various qualitative properties of turbulent states and of the superfluid λ transition are well verified within the limitations of the model; the percolation properties of vortex transitions are exhibited; the differences between superfluid and classical vortex motion are highlighted, as is the importance of topological constraints in vortex dynamics; an earlier model of intermittency is verified.

KEY WORDS: Vortices; transitions; turbulence; superfluids; polymers; percolation.

1. INTRODUCTION

Statistical analyses of turbulent flows and of three-dimensional superfluid dynamics based on vortex lattice representations began to appear almost simultaneously and rely on strikingly similar tools. In the superfluid case, a three-dimensional analog of the Kosterlitz–Thouless renormalization analysis of the λ-transition has been offered by Williams[1] and Shenoy[2]; it relies on Shenoy's ansatz, which assumes a polymerlike structure for a vortex filament near the critical temperature and uses a "magnet" representations; see below. (A "polymer" here and below means "equal probability self-avoiding walk"). In the case of Euler (nonquantum) turbulence, vortices are attracted to an infinite-temperature state whose properties are related in an appropriate model to properties of polymers.[3,4] In both cases, critical exponents are related to the Flory exponent of polymer theory and transition points can be characterized as percolation thresholds;

[1] Department of Mathematics, University of California, Berkeley, California 94720.

0022-4715/94/0800-0835$07.00/0

indeed, a simple model has been used[5] to suggest that the λ-transition and the "turbulent state" can be connected by "universality curves" in a certain phase diagram, and a generalization of the Shenoy–Williams analysis to classical fluids has been offered.[6]

Both analyses as well as their mutual relation are somewhat speculative, and an effort has been made to back them by numerical analyses of lattice vortex models[5,7,8] as well as by XY model calculations[9] and by theoretical analyses of simplified models.[4] In the present paper we pursue the analysis of vortex theory in both the turbulent and the superfluid cases, as well as of their mutual relation, by examining a still-simplified vortex model with long-range interactions in "$2\frac{1}{2}$" dimensions. The numerical method is a fairly standard Metropolis canonical sampling based on a "magnet" representation of vortex filaments. The present model is a useful intermediate step before a full three-dimensional calculation because it is much cheaper to run and the results are relatively easy to interpret; it allows careful convergence studies and bypasses some of the difficulties connected with the gauge freedom of the magnet representation. It also allows for dense collections of vortex filaments, unlike some of the previous work, and with the appropriate caveats, the results appear to be physically relevant.

In two and three space dimensions at positive temperatures, the vortex/magnet lattice model with no topological constraints is dual to the XY model[10] and earlier phase diagrams for that model[11] provide a useful source of comparisons.

The numerical results below support, in the main, the theories quoted above, especially when allowances are made for the unusual dimensionality of the model. The differences between classical and superfluid vortices are highlighted and this contrast constitutes one of the main results of the present paper. The main surprise is that the λ-transition and the turbulent state turn out to live on the same branch of a transition curve in a temperature/chemical potential phase diagram and not on two different branches as suggested in the short-range interaction model of ref. 5. The displacement of that branch from $|T| = \infty$ (classical fluids) to T small (superfluids) appears to be a consequence of the difference in topological constraints between Euler vortex motion and XY-model vortices. This difference may also account for the difference between the values of the standard Flory exponent and the one observed in the XY model. In other words, it is claimed that the equilibrium phase diagrams of the XY model and of the classical vortex system are qualitatively similar; the difference in the precise location of the phase boundaries and in the value of the critical exponents, and thus in the universality class, can be ascribed to the difference in the constraints. To the extent that one can extrapolate from the

XY model to a superfluid vortex system, it is the difference in topological constraints, and not the quantization of the superfluid vortices, that is most responsible for the differences between the latter and classical vortices.

The paper is organized as follows: after a brief review of negative temperatures (needed in the sequel), of earlier work on vortex models of turbulence and of the superfluid transition, and of basic facts about the magnet representation, we present our model, its phase diagram, and other properties. Conclusions are then presented regarding the relation between vortex phase transitions and correlated percolation, and regarding vortex and superfluid phase transitions, intermittency in turbulence, and the non-Euler nature of superfluid vortex motion.

2. NEGATIVE TEMPERATURES

We shall use below negative temperatures T; for the sake of completeness, we begin by a short account, following Landau and Lifshitz.[12] If S is the entropy of an isolated system and E the energy, then $T^{-1} = dS/dE$; in principle, T can be positive or negative.

Suppose two isolated systems, one with energy E_1 and entropy S_1 and one with energy E_2 and entropy S_2, are brought into contact at time $t = 0$. Then $E = E_1 + E_2$ remains constant, while $dS/dt > 0$, where $S = S_1 + S_2$ at $t = 0$. A quick calculation yields

$$0 < \frac{dS}{dt} = \left(\frac{1}{T_1} - \frac{1}{T_2}\right)\frac{dE_1}{dt}$$

(with a symmetric equation involving E_2). If $T_1 > 0$ and $T_2 < 0$, $dE_1/dt > 0$; thus $T < 0$ is "hotter" than $T > 0$. Define $\beta = T^{-1}$; in terms of β, one moves from colder to hotter temperatures as β varies from $+\infty$ to 0 through positive values, and then from 0 to $-\infty$ through negative values. Now, $\beta = 0$ ($|T| = \infty$) is the boundary between $T > 0$ and $T < 0$, and the maximum of $S = S(E)$.

As was discovered by Onsager[13] (modern treatments can be found in refs. 4 and 14), the temperature of a classical vortex system in the plane is usually negative. A similar conclusion was reached in ref. 3 for sparse (i.e., low-density) vortex filament systems in three dimensions, and it was conjectured that the conclusion holds for dense systems as well. On the other hand, superfluid vortices belong to a system with positive temperature T.

Note that if $T > 0$, the Gibbs probability, proportional to $e^{-E/T}$, favors states with low energy E, while for $T < 0$, it favors states with high energy E.

3. SELF-AVOIDING WALKS AND THE EQUILIBRIUM STATISTICS OF CLASSICAL VORTICES

A self-avoiding walk (SAW) on a cubic lattice is a sequence of N lattice bonds such that no site is visited twice (Fig. 1). A family of SAWs is a polymer if all configurations are equally likely. For a polymer, the root mean square average $\langle r_N \rangle$ of the length of the straight line that joins bond 1 to bond N on the SAW satisfies the scaling law $\langle r_N \rangle \sim N^{\alpha}$ for large N, where α is the Flory exponent. Flory's approximate mean-field theory yields $\alpha = 3/5$[15]; modern computing yields $\alpha \sim 0.59$.[16] $D = 1/\alpha$ is the fractal dimension of the polymer.

A lattice vortex is a family of oriented SAWs, each configuration having probability $Z^{-1} \exp(-E/T)$, where Z is the partition function, T is the temperature, and E is the hydrodynamic energy that is produced by a vorticity field supported by the oriented SAW. We shall refer to a configuration of a lattice vortex as a (lattice) vortex filament. Lattice filaments should be closed; this constraint is easily added to what follows and will be disregarded. An appropriate energy can be calculated as follows: the energy of a fluid is $E = \int d\mathbf{x}\, \mathbf{u}^2$, where $\mathbf{u}$ is the velocity. Integration by parts and use of a Green function for a three-dimensional Laplacian yield[17]

$$E = \frac{1}{8\pi} \int d\mathbf{x} \int d\mathbf{x}' \frac{\boldsymbol{\xi}(\mathbf{x}) \cdot \boldsymbol{\xi}(\mathbf{x}')}{|\mathbf{x} - \mathbf{x}'|} \tag{1}$$

where $\boldsymbol{\xi}$ is the vorticity, $\boldsymbol{\xi} = \operatorname{curl} \mathbf{u}$. To find a lattice version of (1), suppose each vortex bond is smeared into a thin tube of vorticity. E can be approximated by

$$E = E_i + N\mu \tag{2}$$

$$E_i = \frac{1}{8\pi} \sum_I \sum_{J \neq I} \frac{\boldsymbol{\Gamma}_I \cdot \boldsymbol{\Gamma}_J}{|I - J|} \tag{3}$$

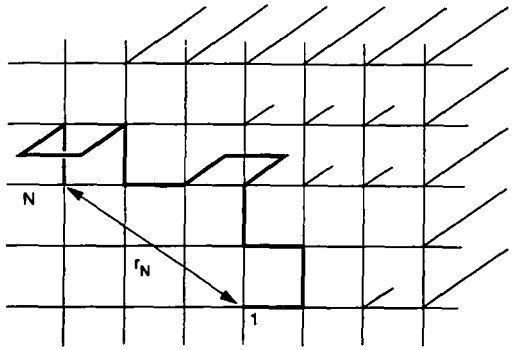

Fig. 1. Self avoiding walk on a lattice.

where I, J are multiindices denoting the origins of bonds occupied by the vortex, Γ_I is a vector pointing in the direction of the bond issuing from I whose magnitude $|\Gamma_I| = \Gamma_I$ equals the circulation of that vortex, $|I-J|$ is the straight-line distance between the bonds issuing from I and from J, and the double sum E_i is the "interaction energy," which one gets from (1) when $\mathbf{x}$, $\mathbf{x}'$ do not belong to the same smeared bond. μ is the contribution to the energy of that part of the Lamb integral (1) where $\mathbf{x}$, $\mathbf{x}'$ belong to the same bond; it is a function of the radius of the smeared bond and of the distribution of vorticity in that bond.[18] We assume all such contributions are equal, and if there are N bonds, their "diagonal" contribution to the energy is $N\mu$. The quantity μ is also known in this context as the "chemical potential." It is analogous to the two-dimensional "chemical potential" of two-dimensional vortex theory,[19] which is an approximation to the chemical potential for sparse vortex systems. This name is a misnomer, as is the other name for μ, "energy per unit length," since the energy associated with a bond depends on all its interactions and, further, a refinement of the lattice takes some of the energy associated with a bond from μ into the double sum E_i. However, in the absence of a better term, we shall call μ the chemical potential without quotation marks or further comment.

The probability of each lattice vortex configuration C is now $P(C) = Z^{-1} \exp[-E(C)/T]$, with $E(C)$ given by (2). If N, μ are constants, both Z and $\exp(-E/T)$ have a factor $\exp(-N\mu/T)$ which cancels out, and only the interaction energy E_i matters. A lattice vortex filament with N finite models loosely a smooth vortex.[3] A vortex imbedded in an Euler flow typically stretches and folds, and N increases. If the mean energy of the vortex remains constant, T decreases. A simple argument shows that a smooth vortex corresponds to $T<0$, and as T decreases, the temperature of the vortex tends toward $|T| = \infty$ ($\beta = 0$). For Euler flow, in the limit $N \to \infty$, $\beta = 0$ is an uncrossable barrier.[3,4] For $T>0$, vortex filaments become very folded, with a fractal dimension 3 ($\alpha = 1/3$); in the presence of a small viscosity, folded vortices reconnect into small loops, and $\beta = 0$ is then the boundary between states with long, smooth vortices and states with small disconnected vortex loops, i.e., a phase transition. This phase transition also looks like a percolation threshold: long vortices for $T<0$, small vortices for $T>0$ (see below). At $\beta = 0$ ($|T| = \infty$), the vortex is a polymer ($E/T = 0$), and one obtains a self-similar spectrum of the Kolmogorov form $E(k) \sim k^{-\gamma}$, with γ the Kolmogorov exponent. The heuristic analysis of ref. 20 together with scaling relations of ref. 21 yield a relation between γ and α, the Flory exponent: $\gamma = 5 - 2/\alpha$. Thus the Flory mean-field value $\alpha = 3/5$ yields the Kolmogorov value of the exponent, $\alpha = 5/3$; the numerical value of the exponent yields a small correction to

this value, in the right direction.[22] The $\beta = 0$ transition point is the only physically relevant equilibrium, as is consistent with general considerations on lattice field models.[23]

One may well wonder why the support of the vorticity has to be self-avoiding. If a lattice vortex covers a lattice bond more than once, the energy (2) is infinite, violating an obvious requirement. On a cubic lattice, a lattice vortex could visit a lattice site more than once without incurring an infinite energy; local interactions vanish because the lattice bonds that meet at a given site are orthogonal. We do not allow repeated site visits both because the local orthogonality is nongeneric in a continuum theory and because the approximation (2) misrepresents the interaction between nearby vortex bonds. A generic vortex with accurate interactions on all scales would associate a large energy with any type of self-intersection.

As always, changes in μ are connected with changes in N. For a classical incompressble fluid, conservation of volume reduces the cross section of a vortex filament as it stretches; an argument given in ref. 8, based on a microcanonical sampling of vortex configurations, shows that stretching, folding, and conservation of volume are incompatible for vortex filaments that remain on a regular lattice. They become compatible on appropriate irregular lattices, giving rise to intermittency. A continuum version of this argument can be found in ref. 22.

The analysis just sketched applies to a single filament or to a sparse collection of filaments. The present paper is a step toward the analysis of dense systems of vortices in three dimensions.

Finally, turbulence in a classical fluid is not an equilibrium process. The relevance of the equilibrium model presented here to classical turbulence is discussed in detail in ref. 4. It is argued there that the establishment of a Kolmogorov spectrum from smooth initial data is an irreversible process; once that spectrum is established, the dynamics in the inertial range should be in the neighborhood of an equilibrium and analyzable by an appropriate variant of the fluctuation-dissipation theorem. The analogous results in two- dimensional turbulence are well-established; in three space dimensions this argument is at variance with well-accepted models, and the reader is welcome to put the word "turbulence" in quotes if he or she desires.

4. SUPERFLUID VORTICES AND THE *XY* MODEL

Another system with vortices is a superfluid away from absolute zero. At temperatures below the critical temperature T_λ a superfluid has elementary excitations that consist of small-diameter vortex loops as well as several kinds of sound waves. Long vortices appear at $T = T_\lambda$, destroying

superfluidity. Long vortices can also appear for $T < T_\lambda$ if the external circumstances are appropriate (e.g., in the presence of rotation or heating).

It is often claimed (see, e.g., ref. 24) that though superfluidity is a quantum effect, superfluid vortices behave like classical vortices. It is further claimed that the main difference between classical and quantum vortex motion is the quantization of superfluid circulation; it can, however, be easily deduced from the convergence theory for vortex approximations (see, e.g., refs. 25 and 26) that under most circumstances, this quantization has a very minor effect. We shall bring out below much more important differences between classical and quantum vortices: They have different topological constraints, different stretching properties, and different ranges of possible temperatures and chemical potentials.

Since the order parameter in the λ-transition is a complex wave function, of constant amplitude for a given T, the superfluid vortex transition is believed to belong in the same universality class as the transition in the XY model, which is a lattice model in which every lattice site is occupied by a vector spin σ of unit modulus, with a Hamiltonian $H = -K\sum \sigma_i \cdot \sigma_j$, where the dot denotes inner product, K is a coupling constant, and the summation is over all sites and all near neighbors. A vortex in the XY model is a plaquette around which the angle between σ and a fixed direction varies by 2π. On a three-dimensional lattice, the centers of these plaquettes can be connected into vortex lines. The XY model is dual to a vortex model,[10] i.e., the partition function can be rewritten as the partition function of a vortex system with a Hamiltonian just like (2), with $\mu = \tilde{\mu}$ a positive number. This dual model does not allow a lattice bond to be covered twice with a positive probability, but does allow a site to be visited twice; in addition, there is no requirement that circulation around vortex lines be preserved, as is necessary in classical flow.

One can generalize the XY Hamiltonian to $H = -K\sum \sigma_i \cdot \sigma_j + \mu N$, where N is the number of vortex points and μ is the added chemical potential (remember that even when $\mu = 0$ in this last formula, the corresponding vortex model has a positive chemical potential). The resulting model has two parameters (T and μ) and its phase diagram has been mapped out for $T > 0$ in two dimensions in the original Kosterlitz–Thouless analysis[19] and in three dimensions by Kohring and Shrock.[11] (Note that in ref. 11 the authors also map out the $K < 0$ region, which, as far as is known, is not dual to a vortex system with $T < 0$.)

A widely believed vortex picture of the transition from a superfluid state to a normal helium state is as follows[1,2,27]: As T increases toward T_λ, the number of vortex excitations increases, and they allay each other's energy through polarization, i.e., large loops arrange smaller loops so as to reduce the energy. Eventually, at $T = T_\lambda$, large loops form and superfluidity

is lost; T_λ thus resembles a percolation threshold for vortex loops (see below). The Shenoy–Williams theory builds a renormalization flow on this picture; the resulting parameter flow is incompletely described (as can be predicted from general principles[27]; to complete its specification, Shenoy introduced an ansatz that relates vortex radius to vortex scale; this ansatz can be related to an assumption that vortex lines at T_λ have structures of polymers; the critical exponents depend on the value of the Flory exponent α. The Shenoy–Williams theory is formulated in magnetization variables, about which more will be said below.

The apparent similarity between the superfluid transition at T_λ and the turbulent state at $|T| = \infty$ is of great interest, in particular because the fractal properties of the turbulent state are better understood, and because a relation between the two states can justify the translation of the Shenoy–Williams theory to the classical case, as in ref. 6. An earlier analysis of this relation, in a model with short-range interactions, was presented in ref. 3.

5. MAGNETIZATION VARIABLES AND VORTEX PERCOLATION

We now present some technical material needed for our model and for explaining the percolation aspects of vortex phase transitions.

The general formulation of magnetization variables and their gauge invariance can be found in ref. 28. Earlier work can be found in refs. 1, 2, 29, and 30. Consider the Euler equation for incompressible flow:

$$\partial_t \mathbf{u} + (\mathbf{u} \cdot \nabla)\mathbf{u} = -\text{grad } p \tag{4}$$

$$\text{div } \mathbf{u} = 0 \tag{5}$$

where $\mathbf{u} = (u_1, u_2, u_3)$ is the velocity, p is the pressure, t is the time, and ∇ is the differentiation vector. At $t = 0$, write $\mathbf{m} = (m_1, m_2, m_3) = \mathbf{u} + \text{grad } q$, where q is an arbitrary scalar. One can veify that $\mathbf{m}$ satisfies

$$\partial_t m_i + (\mathbf{u} \cdot \nabla)\, m_i = -m_j \partial_i u_j \tag{6}$$

where $\mathbf{u} = P\mathbf{m}$, and P is the orthogonal projection that projects arbitrary vector fields on their divergence-free part.[31] Equation (6) is equivalent to the Euler equation (4); since $\mathbf{u}$ is the vector potential for the vorticity $\xi = \text{curl } \mathbf{u}$, the addition of grad q to $\mathbf{u}$ is a gauge transformation; the gauge freedom in Eq. (6) gives rise to the constraint div $\mathbf{u} = 0$.

One can use this gauge freedom to "localize" the vorticity. For example, consider a vortex ring. Its exterior is not simply connected. Pick a surface Σ that spans the ring. In its exterior, which is simply connected,

one can write $\mathbf{u} = -\text{grad}\,\tilde{q}$, and use this $\tilde{q}$ in $\mathbf{m} = \mathbf{u} + \text{grad}\,\tilde{q}$. The $\mathbf{m}$ will be supported on Σ. One can further break Σ into small pieces and calculate the velocity field induced by each piece. A comparison of that velocity field with the velocity field due to a small vortex loop shows that what one has obtained is a representation of a large vortex loop in terms of small vortex loops. The equations of motion for the loops, which can be deduced from (6), form a Hamiltonian system.

The lattice version of this construction is straightforward: Consider a closed lattice vortex. Span it by a union of lattice plaquettes. If the vortex is knotted, it may have to be simplified by simple surgery so that the spanning set of plaquettes does not self-intersect. Attach to each plaquette in the span a "magnet" or "elementary vortex" with the same circulation Γ as the original vortex and oriented so that the union of the elementary vortices yields the original vortex (Fig. 2). Note that vortex bonds may cancel at edges common to two "magnets." The result is the representation of large loops as unions of magnets (the quotation marks are now dropped).

It is obvious that this representation is not unique, just as q above was not unique. This nonuniqueness, a residual gauge freedom, may present interesting problems when a magnet representation is used to calculate entropies and free energies for vortex systems.

The magnet representation gives rise to a percolation problem for vortex filaments. Vortices are edges of clusters of same-orientation magnets. There exist infinitely long vortices when the occupied plaquettes form infinite connected same-orientation clusters while empty plaquettes also form an infinite cluster. What is a connected cluster depends on whether two magnets that touch at one point only form one vortex or two vortices

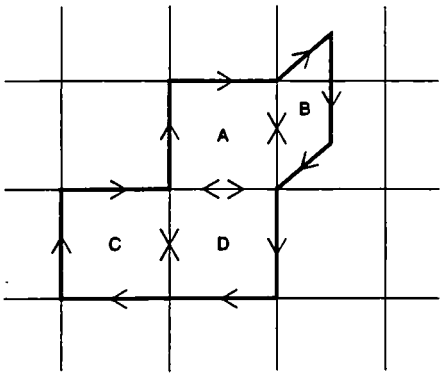

Fig. 2. A vortex as the edge of a magnet cluster.

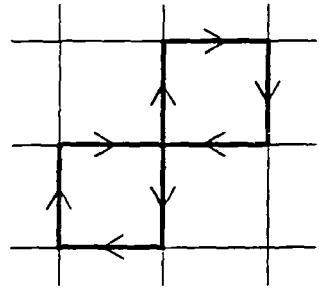

Fig. 3. Neighbors or not?

(Fig. 3); we shall decide this issue when we discuss the numerical results. This decision affects the value of the corresponding Flory exponent (see, e.g., ref. 32).

6. THE $2\frac{1}{2}$-DIMENSIONAL MODEL

We now present our simplified vortex model. All vortex filaments lie in a plane (unlike the vortex filaments in a two-dimensional flow, which are orthogonal to the plane of the motion); $\Gamma = 1$. The velocity field is given by the three-dimensional Biot–Savart law

$$\mathbf{u}(\mathbf{x}) = \frac{1}{4\pi} \sum_I \frac{(\mathbf{x} - \mathbf{x}_I) \times \boldsymbol{\Gamma}_I}{|\mathbf{x} - \mathbf{x}_I|^3} \tag{7}$$

where $\mathbf{x}_I$ is the center of the vortex bond issuing from I, $\mathbf{x}$ is an arbitrary point, and $\times$ denotes a cross-product. This is the discrete version of the usual relation between vorticity and velocity in three dimensions; $\mathbf{u}(\mathbf{x})$ has typically three nonzero components. The energy of the system is given by (2). Both (7) and (2) are based on the three-dimensional Green function. The use of a three-dimensional Green function and the presence of vortex filaments can be expected to endow the model with properties intermediate between those of two-dimensional and three-dimensional models, as will indeed turn out to be the case, hence the name "2.5 dimensional model."

The vortex configurations in their plane are generated by magnets of one orientation. We shall refer to the resulting vortex filaments, the edges of magnet clusters, as "macroscopic vortices." It is easy to see that even when the magnets all have one orientation (say, counterclockwise), the resulting macroscopic vortices can have either clockwise or anticlockwise orientation (for example, assume all plaquettes in the plane but one are occupied). However, some possible macroscopic vortex configurations

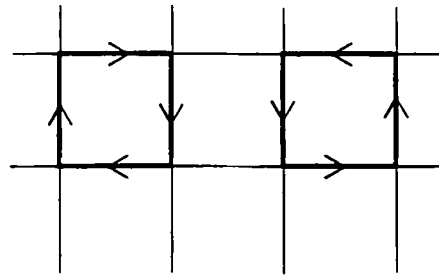

Fig. 4. A vortex configuration that cannot be built up with one-orientation magnets.

cannot be generated by one-orientation magnets (see, for example, Fig. 4). To make sure that all macroscopic vortices can appear, one has to accept that some of them can be generated in more than one way, and the choice has been made not to do so. All the magnets have circulation 1, and thus all the macroscopic vortices have circulation 1. Thus, in this model, the nonuniqueness of **m** can be circumvented.

Consider in particular an $m \times m$ sublattice in the plane, with bond length 1. The energy of this lattice is, as in (2), $E = \sum \Gamma_I \cdot \Gamma_J / |I - J| + \mu N$, where N is the number of occupied bonds (remember that the canceled vortices between occupied plaquettes are not counted). μ is the chemical potential. The problem has two physical parameters: T (or $\beta = T^{-1}$) and μ.

The problem presented by the boundary condition at the edges of a finite sublattice is severe: the Green function decays like $1/m$, while the boundary length grows like m. If the correlation functions decay rapidly, this may not matter, and if the correlation functions decay slowly, they may do so even if the domain is finite. What we did was make the vorticity periodic and cut the Green function off at separations greater than $m/2$, so that each vortex bond interacts only with one other bond, and not with an infinite array of images. We shall check that the results are independent of m, and thus that the approximation involved is presumably harmless.

The model just formulated will be solved by a straightforward Metropolis sampling, in which the steps consist of an addition or subtraction of individual magnets. Each such move changes the status of four vortex bonds; the corresponding interaction energies and chemical potentials must be added or subtracted, which costs $O(m^2)$ operations per move. The number of moves for convergence is relatively modest—a few thousands of steps for $m = 20$. All quantities we shall calculate converge rapidly in m: none of the results below changes by more than the modest statistical error when m increases beyond 20, and some remain substantially unchanged as m goes down to $m = 6$ (!), in agreement with the observation in ref. 11 that

a relatively small lattice is sufficient to provide information about the phase diagram. All the results below come from runs with either $m = 20$ or $m = 30$. The errors in Fig. 5 and 12 are negligible, i.e., the uncertainty is comparable with the thickness of the lines in the figures; finite-size scaling adds little. The error bars in Fig. 7 are based an a statistical analysis only; there is presumably an added systematic error due to the finite size of the lattice. This error makes it impossible to decide whether the specific heat has a singularity at the transition. Note, however, that the location of the transition is determined with great accuracy.

Note that in the phase diagram the factor $(8\pi)^{-1}$ in the energy has been omitted, thus redefining the temperature in the case of the classical fluid; the absence of this factor is in agreement with usual practice in the case of the XY model.

7. THE PHASE DIAGRAM

The numerical calculation produces the phase diagram in the (β, μ) plane shown in Fig. 5. Note that the β axis is labeled so that the temperature increases from left to right; $T > 0$ is on the left. Phase I is a "solid" phase, as shown in Fig. 6a, that exists for T low enough and μ low enough, when the interaction energy E_i is at a minimum which produces this phase. Another branch of phase I is produced for μ large and $T < 0$, $|T|$ large, when the high energy μN can overwhelm any negative contribution from E_i. Phase II is a "gas" phase (Fig. 6b). Vortex loops are few and far between. Phase II is produced for T small enough and μ large enough.

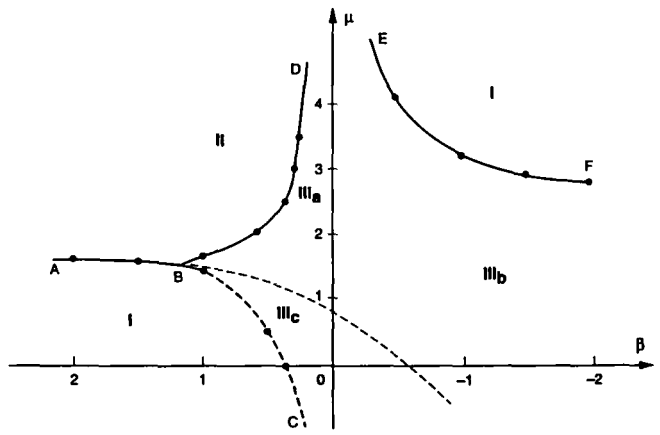

Fig. 5. The phase diagram.

Phase III is the intermediate "vortex liquid" phase, and has several subregions. In region III_c the mean energy $\langle E \rangle$ is negative, which is nonphysical. In region III_a (Fig. 6c) the vortex system is more disordered than in region III_b (Fig. 6d); the transition between III_a and III_b is gradual.

The transitions between phases I and III, II and III, and I and II are second order, in the sense that either the specific heat has a singularity or its derivative with respect to T does, as is the case in three space dimensions,[11] but not in two.[19] To show the nature of the transition, we exhibit in Fig. 7 the specific heat C as a function of μ for $\beta = 1$. The sharp peaks are well defined, and the $I \to III$ and $III \to II$ transitions are well separated.

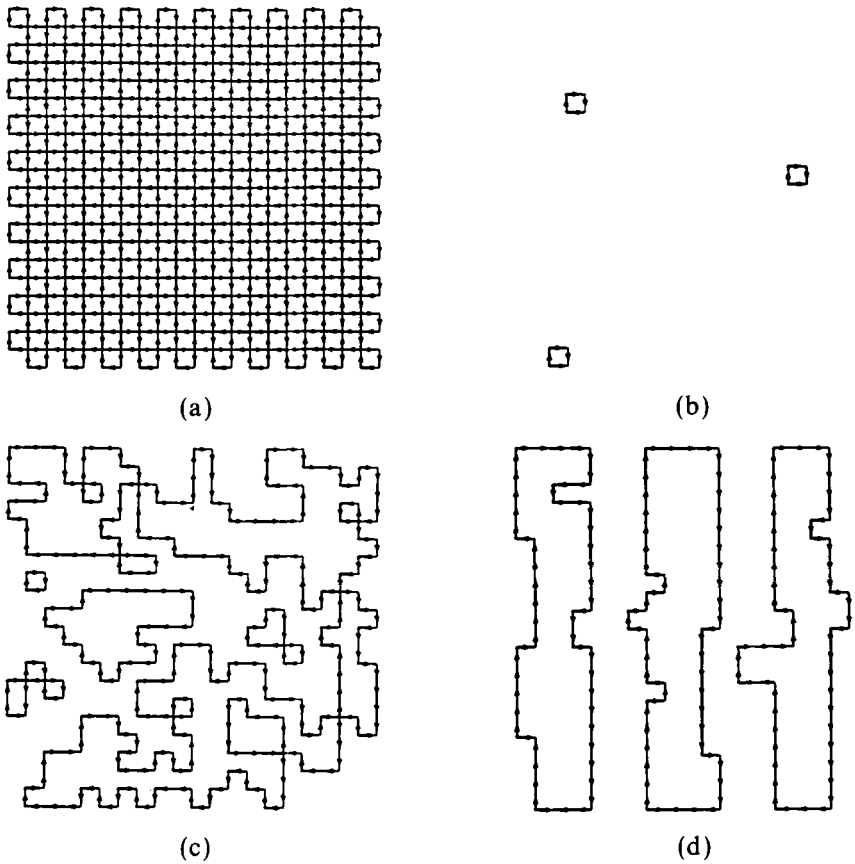

Fig. 6. The phases: (a) "solid" I; (b) "gas" II; (c) "liquid" III_a; (d) "more organized liquid" III_b.

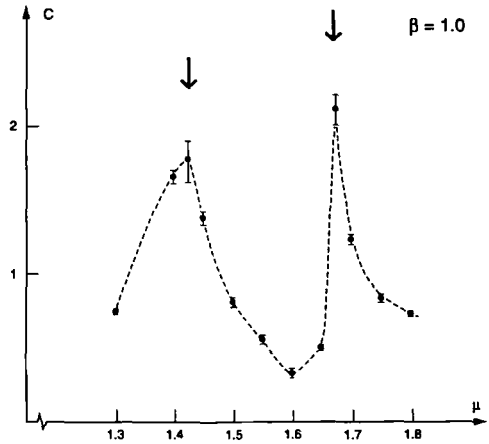

Fig. 7. Specific heat as a function of chemical potential, $\beta = 1$.

Note that the "liquid" phase transition $\widehat{BD}$ in Fig. 5 is located in the $T > 0$ region. In the region between the arc $\widehat{BD}$ and the μ axis longer vortices can exist because interactions cancel each other, i.e., polarization and screening appear. The transition along $\widehat{BD}$ fits the description of the λ-transition. The boundary $\widehat{AB}$ of the "solid" phase in the $T > 0$ half-plane presumably has a horizontal asymptote $\mu = \tilde{\mu}$; if there is an analogous phase transition in three dimension, then $\tilde{\mu} \leqslant \mu_0$, where μ_0 is the chemical potential in the vortex model that corresponds to zero added chemical potential in the XY model. There is no direct way to evaluate μ_0 in $2\frac{1}{2}$ dimensions. We shall argue below that the arc $\widehat{BD}$ also corresponds to the phase transition in the classical vortex systems; this transition has been displaced from the line $\beta = 0$ by the assumptions in our model, which allows self-intersection (see Fig. 6). Note that in three dimensions the arc analogous to the arc $\widehat{BD}$ crosses the μ axis,[11] but its analog in two dimensions does not.[19]

There may be another transition in the region $T < 0$, $\mu < 0$; it is of no physical interest and has not been mapped out.

In Fig. 8 we reproduce the lines of constant $\langle E \rangle$ in the (β, μ) plane (note the change of scale). On the whole, if T decreases (allowing for the unusual meaning of this phrase when $T < 0$) and $\langle E \rangle$ remains constant, μ must increase, as is heuristically obvious.

In Fig. 9 we display the average bond occupation fraction s (number of vortex legs divided by m^2). In phase I, when all the bonds are occupied, $s = 2$. Along the μ axis, the model is not well defined, but one can check that the limit of the model as $\beta \to 0$ from either side is indistinguishable

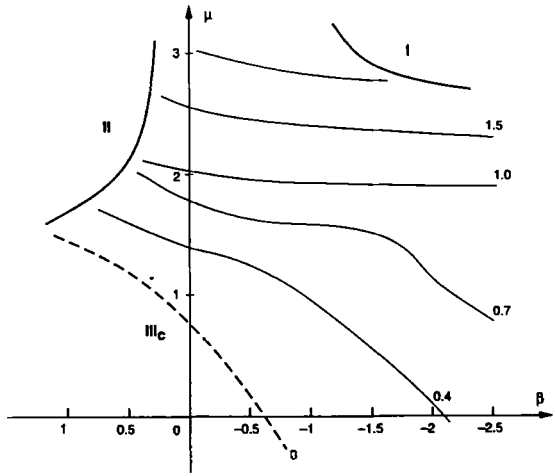

Fig. 8. Constant-energy curves in phase diagram.

from what one would get by placing magnets on the plaquettes, with a probability $p = 1/2$ of any plaquette being occupied and each plaquette being independent of the others. In this case, $s = 0.91$ ($s \neq 1$ because of leg cancellation between neighboring plaquettes). Except for large μ, s increases as T decreases or as μ increases, as intuition would indeed suggest.

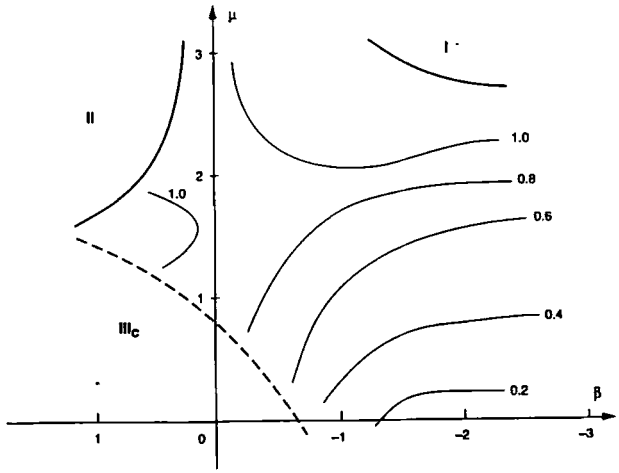

Fig. 9. Curves along which the fraction of occupied bonds is constant.

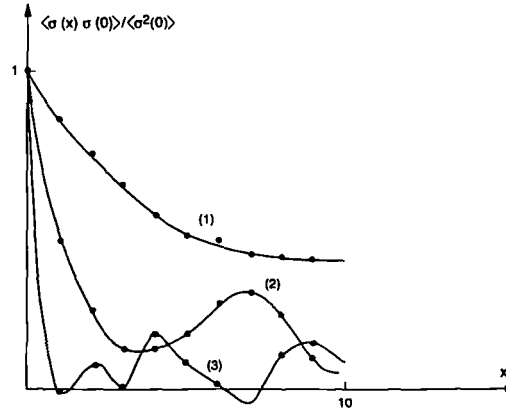

Fig. 10. Spin–spin correlation functions: (1) $\beta = 1$, $\mu = 2$ (phase II); (2) $\beta = -2$, $\mu = 1$ (phase III_b); (3) $\beta = -0.1$, $\mu = 1.75$ (phase III_a).

No effort has been made to determine the critical exponents at the transitions, since they are not likely to be independent of the dimensionality of the problem.

In Fig. 10 we display the "spin–spin" correlation function at several pairs of values (β, μ). In a two-or three-dimensional XY model, a phase ϕ (angle between spin and a fixed direction) is defined at every lattice point, with grad $\phi = \mathbf{u}$, $\mathbf{u}$ is the local velocity field. In $2\frac{1}{2}$ dimensions we define, by analogy, a spin $\sigma = (u_3 + \varepsilon)/|u_3 + \varepsilon|$ if $u_3 + \varepsilon \neq 0$, and $\sigma = 0$ if $u_3 + \varepsilon = 0$, where u_3 is the velocity out of the plane as given by (7) and ε is a small parameter (here, $\varepsilon = 10^{-6}$). Then σ is either $+1$ or -1. The sign of σ changes as vortices are crossed, in analogy to the effect of vortices on ϕ; ε is here to make sure that if there are no vortices, all the spins are aligned. The correlation function $S(x)$ at x is $S(x) = \langle \sigma(x)\, \sigma(0) \rangle / \langle \sigma^2(0) \rangle$, where the origin is arbitrary, and x is less than $m/2$ to avoid edge effects on the periodic lattice. In Fig. 10 we summarize the variation in $S(x)$ as one moves in the phase diagram. Curve 1 corresponds to $\beta = 1$, $\mu = 2$, i.e., a point in the vortex "gas" phase; one can see long-range order. Curve 3 corresponds to $\beta = -0.1$, $\mu = 1.75$ (region III_a); the order is lost. Curve 2 corresponds to $\beta = -2$, $\mu = 1$ (region III_b); some order is recovered, in agreement with what we know from the sparse vortex model,[3] where order is found for $T < 0$.

8. PHASE TRANSITIONS AS PERCOLATION THRESHOLDS; THE FLORY EXPONENT

Both the λ-transition and the turbulent state were described earlier as percolation thresholds, in which large organized vortices give way to

isolated vortex loops (or vice versa, depending on which side one is coming from). In refs. 5 and 33 the phase transition was identified by percolation properties. Does this identification of the transition along the $\widehat{BD}$ arc of Fig. 5 hold up in our model?

In site percolation problems, a set of occupied sites that can be reached from one of them by stepping only on occupied sites is called a cluster; a similar definition holds for bond percolation. In independent percolation, in which sites or bonds are occupied with probability p and the probabilities of two sites being occupied are independent of each other, the probability P that there exists an infinite cluster is 0 for $p < p_c$ and 1 for $p > p_c$; p_c is the percolation threshold. Connections between polymer theory and percolation have been explored, e.g., in ref. 34. Our vortices here have boundaries of clusters in a "correlated" plaquette percolation problem, where the probabilities of two plaquettes being occupied are not independent.

On a finite $m \times m$ lattice, the probability of a numerically generated cluster in an independent percolation problem crossing the lattice from side to side is near 0 for $p < p_c - \varepsilon(m)$ and near 1 for $p > p_c + \varepsilon(m)$, where ε is a small quantity that decays with m. At $p = p_c$, one might expect a probability q, $0 < q < 1$, that a cluster cross the lattice, as a result of edge effects. Efficient algorithms for calculating p_c accurately in independent percolation problems exist, but do not readily generalize to correlated percolation.

The presence or absence of vortex percolation (i.e., of very long vortices) depends on what one defines as "neighboring plaquettes." If two plaquettes are viewed as neighbors only when they have a common bond, there will be very few large clusters. Here we use the same convention as was made in ref. 5: Suppose the plaquettes have centers at (i, j), i, j integers. The plaquette at (i, j), $i + j$ even, is connected to the plaquettes at $(i+1, j+1)$ and $(i-1, j-1)$ (to the northeast and southwest), but is not connected to the plaquettes at $(i+1, j-1)$ (southeast) or $(i-1, j+1)$ (northwest). The opposite is assumed when $i + j$ is odd. One can verify that the resulting percolation problem is equivalent to a bond percolation problem on a square lattice with $p_c = 1/2$. Other connections can be found that also lead to $p_c = 1/2$. Vortex lines (edges of clusters) with our convention look as in Fig. 11.

In Fig. 12 we display the variation of the probability P that there exists a vortex that crosses the $m \times m$ lattice as one crosses the $\widehat{BD}$ transition line. In the example, $\mu = 1.75$ and β varies. The transition, marked by an arrow, is near $\beta = 0.85$. We have $P = 0$ in the "gas" phase I and $P > 0$ in phase III. The probability P remains less than 1 for all β in phase III; indeed, one expects $0 < P < 1$ on the line $\beta = 0$ when the percolation is independent with $p = p_c = 1/2$. It is as if the whole region III were at the

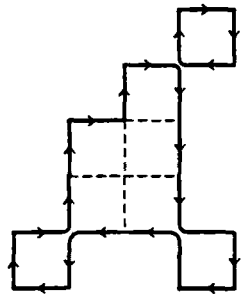

Fig. 11. Magnet cluster edges according to the convention in the text.

threshold, with the arc $\widehat{BD}$ as the threshold of the threshold. The characterization of the transition by means of a percolation property survives; the vortices have an increasing probability of crossing the lattice as $\beta \to -\infty$ or $\mu \to 0$.

The Flory exponent α (which can be defined here as the inverse of the fractal dimension of the percolating vortices) is calculated at the transition line as 0.55 ± 0.02, a fair agreement with the value $4/7 \cong 0.57\ldots$ of independent percolation.[35] However, this determination is not accurate, and one should not jump to conclusions. One can readily estimate the amount of work required to yield several good digits in α and see that it is beyond reach at the moment.

This exponent is below the $\alpha = 0.75$ value for two-dimensional polymers, as can be expected from the fact that the vortices can self-inter-

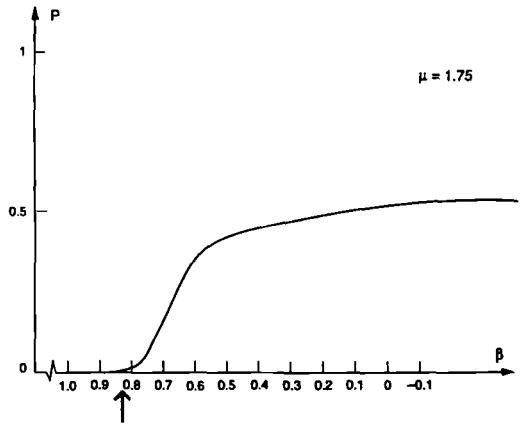

Fig. 12. Percolation probability as a function of chemical potential as one crosses a phase transition line.

sect. The topology of the vortices is that of XY-model vortices (see below), and this observation is in qualitative agreement with the numerical observations of Epiney,[9] who found an α markedly below the Flory value for XY vortices in three dimensions. Thus the Shenoy ansatz[2] may have to be slightly revised.

9. CORRESPONDENCE WITH THE SPARSE CLASSICAL VORTEX MODEL; INTERMITTENCY

We now compare the results obtained here with the sparse vortex model.[3,4,20] In the sparse model, as the number of vortex bonds increases with energy remaining finite, the temperature T decreases; this is the case here, too (contrast Fig. 8 with Fig. 9). As a consequence, if a vortex "liquid" is imbedded in a Eulerian flow, in which vortex lines are stretched, the temperature of the vortex will decrease until the transition line $\widehat{BD}$ is reached. The system cannot go any further without energy loss or a discontinuity in the number of vortex legs. This situation is discussed at length in ref. 4.

Along the constant energy line, μ increases as s, the fraction of bonds that are occupied, increases. The relation $\mu = \mu(s)$ is determined by the statistics. In a classical fluid, μ increases as the vortices are stretched, because incompressibility reduces vortex cores and increases the corresponding energy. Under plausible assumptions on the distribution of vorticity in a vortex cross section, one can also calculate $\mu = \mu(s)$, and the two functions of s do not coincide. This observation has been made before, in the context of a microcanonical model.[8] The conclusion is that to accommodate a constant or slowly varying energy with vortex stretching, vorticity must stretch into a nonuniform grid, creating nonuniformly active subregions and thus intermittency.[4,8,22]

The main differences between the model here and the sparse model are (i) the phase transition has shifted from the $\beta = 0$ line into the $\beta > 0$ region and (ii) the transition from order to disorder is more abrupt in the sparse model. Both phenomena are probably the consequences of the freedom to self-intersect that the vortex lines have here; circulation is no longer a constant of the Monte Carlo "motion" and reconnection is freely allowed. Reconnection is well known to mitigate energy variations (see, e.g., ref. 36). To the extent that the model here is a better cartoon of XY vortices than of hydrodynamical vortices, it highlights the differences between classical and quantum vortices.

10. CONSEQUENCES FOR THE DYNAMICS OF SUPERFLUID VORTICES

Our model, though it has a peculiar dimensionality and fails to exhaust all vortex configurations, provides a qualitative description of superfluid vortex motion if that motion can be assumed to be in some correspondence with the behavior of XY-model vortices.

Superfluid systems can maintain a constant temperature and the behavior of their vortices is affected, and indeed controlled, by the temperature of the ambient fluid. Superfluid vortices are then coupled to the molecular degrees of freedom of the fluid, presumably through vortex/wave interactions; thus vortex stretching is limited (see Fig. 9). This conclusion agrees well with the visual observation of superfluid vortices, which look smooth, and with standard results on their stretching behavior; for example, the rate of change dL/dt of the line length L per unit volume is $dL/dt \sim L$ in a classical fluid,[4] while it is $\sim L^{3/2}w$ in a superfluid, where w is a "counterflow" velocity that vanishes at T_λ.[37]

These obsrvations raise the question of what equations of motion describe the temporal evolution of superfluid vortices. The Euler equations for incompressible flow are not compatible with constant T, and we have already pointed out above that the quantization of circulation is not a major effect. The important qualitative difference between classical and superfluid vortices is that the latter do not have to move at the velocity of the fluid that surrounds them.[37] Schwarz,[38] following Feynman, has proposed that superfluid vortex motion can be described by the local self-induction approximation with Hall–Vinen friction and reconnection added. Unfortunately, his paper is marred by numerical errors and an irrelevant, and erroneous, claim that the self-induction approximation approximates Euler (i.e., classical) vortex motion.[39,40] The self-induction approximation preserves arc length and thus forbids stretching, and may well be a better basis for a phenomenological description than Euler vortex motion. Reconnection, not allowed by the Euler equations, has been seen to be an important feature of XY vortices and thus presumably of superfluid vortices (as well as of viscous vortices, not discussed here[4]). It likely that the correct description would be something intermediate between Euler vortex motion and self-induction motion; possible candidates can be found, e.g., in Klein and Majda.[41] We shall present an exhaustive analysis of the possibilities as well as analysis of the effect of Hall–Vinen friction in a separate publication.

11. GENERAL CONCLUSIONS

We have presented a simplified model of vortex equilibria on a lattice which has reasonable qualitative properties and provides information

about the properties of the "polymeric" models of turbulence as well as a useful basis for speculation on superfluid vortex motion.

The methodology can be extended to three-dimensional vortex equilibria as well as to other defect-dominated statistical phenomena, as will be shown in subsequent work.

ACKNOWLEDGMENTS

This work was partially supported by the Applied Mathematical Sciences subprogram of the Office of Energy Research, U.S. Department of Energy, under contract DE-FG02-88ER25053, and by the National Science Foundation, under grant DMS-9100383.

REFERENCES

1. G. Williams, *Phys. Rev. Lett.* **59**:1926 (1987).
2. S. R. Shenoy, *Phys. Rev. B* **40**:5056 (1989).
3. A. J. Chorin, *Commun. Math. Phys.* **141**:619 (1991).
4. A. J. Chorin, *Vorticity and Turbulence* (Springer, New York, 1994).
5. A. J. Chorin, *J. Stat. Phys.* **69**:67 (1992).
6. A. J. Chorin, *J. Comput. Phys.* **107**:1 (1993).
7. B. Chattopadhyay, M. Mahato, and S. Shenoy, Vortex loop crinkling in the three-dimensional XY model: Numerical evidence in support of an ansatz, *Phys. Rev. B*, in press.
8. A. J. Chorin, *Commun. Pure Appl. Math.* **39**(Spec. Iss.):S47 (1986).
9. J. Epiney, 3D XY model near criticality, Diploma Thesis, ETH, Zurich (1990).
10. R. Savit, *Rev. Mod. Phys.* **52**:453 (1980).
11. G. Kohring and R. Shrock, *Nucl. Phys. B* **288**:397 (1987).
12. L. Landau and E. Lifshitz, *Statistical Physics*, 3rd ed., Part 1 (Pergamon Press, New York, 1980).
13. L. Onsager, *Nuovo Cimento* (Suppl.) **6**:279 (1949).
14. G. L. Eyink and H. Spohn, *J. Stat. Phys.* **70**:833 (1993).
15. P. G. de Gennes, *Scaling Concepts in Polymer Physics* (Cornell University Press, Ithaca, New York, 1971).
16. N. Madras and A. Sokal, *J. Stat. Phys.* **50**:109 (1988).
17. H. Lamb, *Hydrodynamics* (Dover, New York, 1932).
18. A. J. Chorin, *Commun. Math. Phys.* **114**:167 (1988).
19. J. Kosterlitz and D. J. Thouless, *J. Phys. C: Solid State Phys.* **6**:1181 (1973).
20. A. J. Chorin and J. Akao, *Physica D* **52**:403 (1991).
21. J. Akao, Scaling relations for fractal objects, Department of Mathematics, University of California, Berkeley, California (1993).
22. A. J. Chorin, *Phys. Rev. Lett.* **60**:1947 (1988).
23. D. Callaway, *Contemp. Phys.* **26**:1, 95 (1985).
24. D. Tilley and J. Tilley, *Superfluidity and Superconductivity* (Adam Hilger, Bristol, 1986).
25. O. Hald, *SIAM J. Num. Anal.* **16**:726 (1979).
26. J. T. Beale and A. Majda, *Math. Comp.* **39**:1 (1982).
27. B. I. Halperin, *Statistical Mechanics of Topological Defects*, Les Houches 1980 Lectures Notes (North-Holland, Amsterdam, 1981).
28. T. Buttke, Lagrangian numerical methods which preserve the Hamiltonian structure of incompressible fluid flow, *Commun. Pure Appl. Math.*, in press.

29. V. I. Oseledets, *Russ. Math. Surv.* **44**:210 (1989).
30. P. H. Roberts, *Mathematica* **19**:169 (1972).
31. A. J. Chorin and J. Marsden, *A Mathematical Introduction to Fluid Mechanics* (Springer-Verlag, Berlin, 1979, 1990, 1992).
32. T. Grossman and A. Aharony, *J. Phys. A* **20**:L1193 (1987).
33. A. G. Bershadski, *Usp. Fiz. Nauk* **160**:189 (1989); *Sov. Phys. Usp.* **33**:1073 (1990).
34. A. Coniglio, N. Jan, I. Majid, and H. E. Stanley, *Phys. Rev. B* **35**:3617 (1987).
35. H. Saleur and B. Duplantier, *Phys. Rev. Lett.* **58**:2325 (1987).
36. A. J. Chorin, *J. Comput. Phys.* **91**:1 (1990).
37. H. Hall and W. Vinen, *Proc. R. Soc. Lond. A* **238**:215 (1956).
38. K. Schwartz, *Phys. Rev. Lett.* **49**:283 (1982).
39. T. Buttke, *J. Comput. Phys.* **76**:301 (1988).
40. T. Buttke, *Phys. Rev. Lett.* **59**:2117 (1987).
41. R. Klein and A. Majda, *Physica D* **49**:323–352 (1991).